PHYSICAL REVIEW B VOLUME 56, NUMBER 14 1 OCTOBER 1997-II

Local Jahn-Teller distortion in $La_{1-x}Sr_xMnO_3$ observed by pulsed neutron diffraction

Despina Louca* and T. Egami
Department of Materials Science and Engineering and Laboratory for Research on the Structure of Matter, University of Pennsylvania, Philadelphia, Pennsylvania 19104

E. L. Brosha, H. Röder, and A. R. Bishop
Los Alamos National Laboratory, Los Alamos, New Mexico 87545
(Received 18 July 1997)

The atomic pair-density function of $La_{1-x}Sr_xMnO_3$ ($0 \leqslant x \leqslant 0.4$) obtained by pulsed neutron diffraction indicates that their local atomic structure significantly deviates from the average structure, and that the local Jahn-Teller (JT) distortion persists even when the crystallographic structure shows no JT distortion. In the paramagnetic insulating phase doped holes form one-site small polarons, represented by the local absence of JT distortion. The polarons become more extended at low temperatures, but local distortions are found even in the metallic phase. The role of polarons in the phase transitions in transport and magnetic properties are discussed. [S0163-1829(97)50638-2]

The manganese-based perovskite compounds $La_{1-x}A_xMnO_3$ (where A stands for Sr, Ba, Ca, or Pb)[1–3] have recently received considerable interest because of the discovery of their colossal magnetoresistance (CMR).[4] Over certain ranges of composition a transition from a paramagnetic (PM) insulator to a ferromagnetic (FM) metal is observed as a function of temperature and magnetic field. While the connection between ferromagnetism and electrical conduction was explained earlier in terms of the double exchange (DE) mechanism,[5–7] more recently Millis *et al.*[8] pointed out that the DE model is inadequate for explaining many of the observed properties and proposed lattice involvement in the mechanism, possibly via polaron formation. Recent experiments generally support this idea,[9–16] however, the subject is still highly controversial, and no convincing structural evidence of polaron formation has been provided.

In this paper, we describe the results of our pulsed neutron scattering experiments on powder samples of $La_{1-x}Sr_xMnO_3$ ($0 \leqslant x \leqslant 0.4$). Through the pair-density-function (PDF) analysis,[17,18] we demonstrate that the *local* structure in this system is quite distinct from that suggested by the crystallographic structure. We show that the Jahn-Teller (JT) distortion is *locally* present in the metallic as well as insulating phases, and suggest a direct link between the JT distortions and the polarons. The presence of lattice polarons in manganites was suggested by Billinge *et al.* in the PDF study of $La_{1-x}Ca_xMnO_3$.[11] However, based upon the results on the temperature dependence of the PDF they concluded that the polarons are of a conventional breathing type and are unrelated to the JT distortion. The present results point to the direct connection between them. In addition we observed local distortions in the metallic phase at low temperatures which pose a question on the current homogeneous picture of the metallic state.

The powder samples were prepared by the solid-state reaction method. Ceramic samples were formed from $SrCO_3$, MnO_2, and La_2O_3 between 1250 and 1300 °C, and were annealed in a controlled atmosphere at 1000 °C to ensure oxygen stoichiometry. The pulsed-neutron powder-diffraction data were collected using a time-of-flight technique with the glass-liquid-amorphous diffractometer (GLAD) at the Intense Pulsed Neutron Source (IPNS) of the Argonne National Laboratory. The data were corrected for background, absorption, incoherent scattering, multiple scattering, and inelastic scattering (Placzek correction) to obtain the structure function $S(Q)$ up to the momentum transfer, Q, of 40 $Å^{-1}$. The PDF, $\rho_0 g(r)$, is a real-space representation of atomic density correlation calculated by Fourier transforming $S(Q)$, and has been quite effective in determining the local atomic structure of amorphous as well as crystalline materials.[17,18] The multiple-scattering correction procedure for the GLAD spectrometer was carefully calibrated so that it gives a correct PDF for crystalline Ni, $SrTiO_3$, and MnO powders.

The structure of $LaMnO_3$ has monoclinic ($P2_1/c$) symmetry.[19] The Mn^{3+} $3d$ states are split by the cubic crystal field to the t_{2g} and e_g levels, and the singly occupied e_g level is further split by the Jahn-Teller effect that leads to an elongation of the MnO_6 octahedron. Because of this distortion the Mn-O bond lengths within the octahedron are grouped into two, those ranging from 1.87 to 2.00 Å corresponding to the short bonds (four per each Mn), and from 2.11 to 2.22 Å for the long bonds (two per each Mn).[20] This split is clearly seen in the PDF determined for $LaMnO_3$ (Fig. 1) as the first negative peak at 1.93 Å representing the short bonds and the second negative peak for the long bonds around 2.2 Å. Note that these peaks are negative because of the negative neutron scattering length of Mn. The neutron PDF's at $T=10$ and 300 K are in excellent agreement with the model PDF calculated for the $P2_1/c$ structure[20] also shown in Fig. 1. The model PDF of the crystallographic structure is originally composed of many δ functions. This is convoluted with a Gaussian function to represent quantum and thermal lattice vibrations with a full width at half-maximum of 0.14 Å, which is similar to the value that best describes the PDF of MnO, and is consistent with the Debye temperature of $La_{0.8}Ca_{0.2}MnO_3$.[21] The error in the PDF estimated from the statistical error[18] is about 0.012 $Å^{-3}$ in this range.[22]

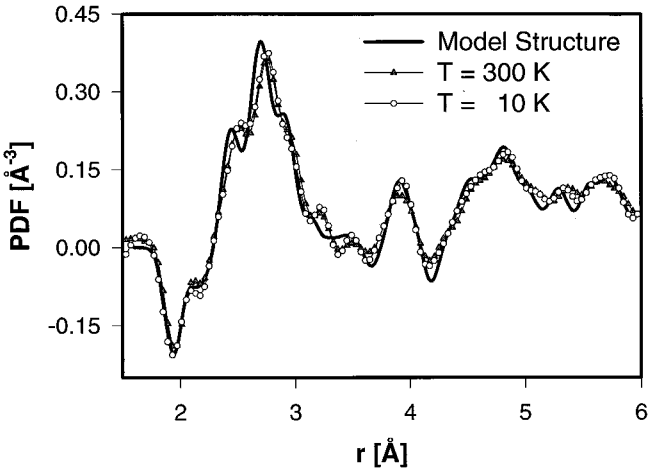

FIG. 1. The PDF's of $LaMnO_3$ at room temperature and at 10 K compared to the PDF calculated for the crystallographic structure. The experimental and model PDF's show excellent agreement.

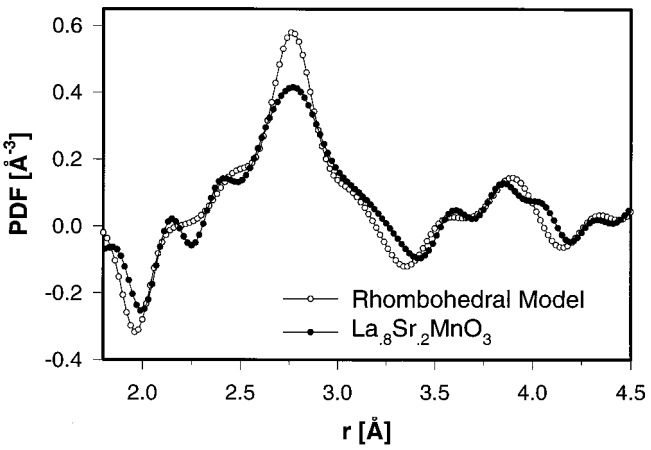

FIG. 3. The PDF's of $La_{0.8}Sr_{0.2}MnO_3$ compared with the PDF calculated from the crystallographic rhombohedral structure (Ref. 20). The Mn-O peak at 2.25 Å is present in the experimental PDF but not in the calculated PDF.

Figure 2 shows the PDF's of $La_{1-x}Sr_xMnO_3$ at 300 K for $x=0.08$ (monoclinic), $x=0.15$ (orthorhombic, *Pbnm*), and at 320 K for $x=0.20$ (rhombohedral, *R3C*). At these temperatures the samples are all paramagnetic and insulating. It should be noted that the small negative peak around 2.2 Å that corresponds to the long Mn-O distance persists with little change in spite of the variation in the lattice structure. In Fig. 3 the PDF of the $x=0.2$ sample is compared with the model PDF calculated for the rhombohedral structure with $x=0.2$.[20] The JT peak at 2.2 Å is clearly present in the experimental PDF, while it is absent in the calculated PDF. The positions of the two Mn-O peaks shown in Fig. 4 indicate that they are basically independent of composition up to $x=0.3$. Thus the magnitude of the local JT distortion is unchanged by Sr doping, and the JT distortion is *locally* present even in the rhombohedral phase beyond $x=0.16$. It is most likely that the orientation of the local JT distortion varies from site to site in the rhombohedral phase, and the symmetry is maintained only in average. The presence of local JT distortions were suggested also by the recent extended x-ray-absorption fine structure (EXAFS) measurements[12,15] and the high-resolution electron microscopy observations.[23] However, one of the two EXAFS results[12] yields an unphysically long Mn-O bond length (2.5 Å) while the other[15] sees very small distortion, which is inconsistent with the large Debye-Waller factor.[24]

While the peak positions are largely independent of composition, the intensities of the peaks vary with composition. This is clearly demonstrated by the PDF's in Fig. 2 and those of the 17.5, 20, and 40 % samples at $T=10$ K, all in the metallic phase, shown in Fig. 5. While the first Mn-O peak at 1.95 Å becomes stronger with x, the second Mn-O peak at 2.25 Å becomes weak, and disappears almost completely for $x=0.4$ at 10 K. The area of the first Mn-O peak is related to the number of short Mn-O bonds, $N_{\text{Mn-O}}$ shown in Fig. 6 as a function of composition. The value of $N_{\text{Mn-O}}$ was deter-

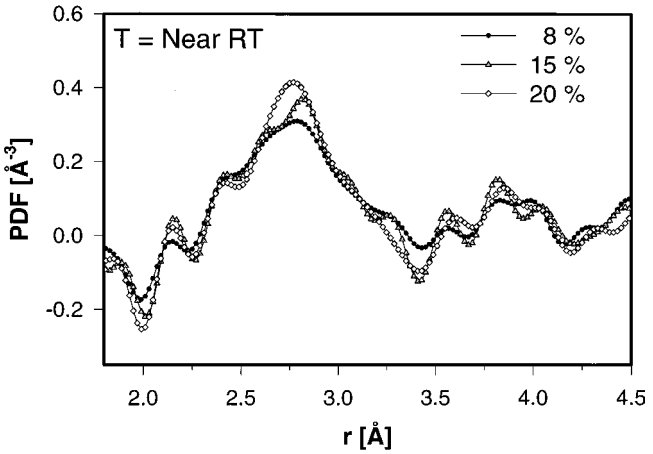

FIG. 2. The PDF's of $La_{1-x}Sr_xMnO_3$ for $x=0.08$ and 0.15 at 300 K, and 0.20 at 320 K. All samples are paramagnetic insulators. It can be seen that the composition dependence of the local structure is relatively small.

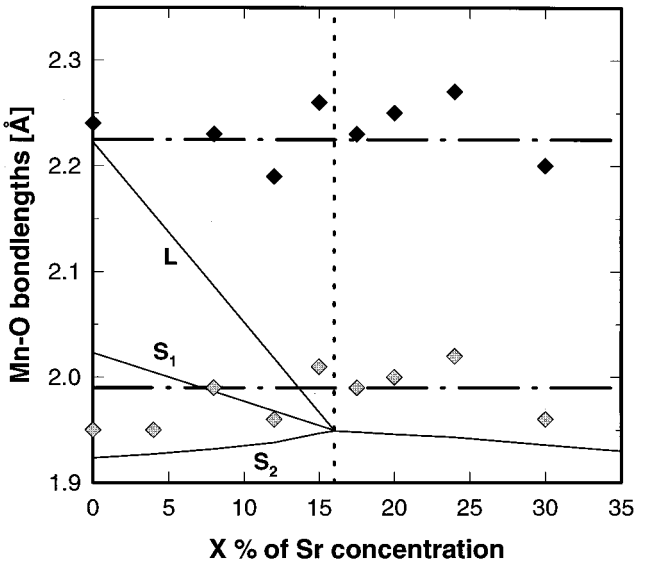

FIG. 4. The Mn-O bond lengths as determined from the PDF (triangles) compared to those deduced from the lattice constants of the crystal structure (solid lines L, S_1, and S_2) (Ref. 26). Note that the local JT distortion is present even in the rhombohedral phase.

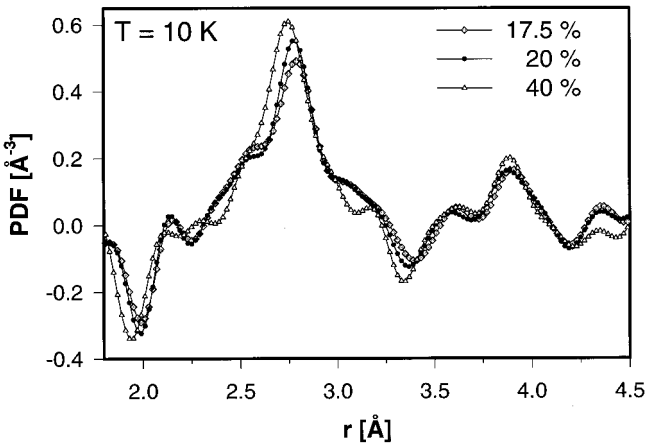

FIG. 5. The PDF for $x=0.175$, 0.2, and 0.4 at $T=10$ K, all in the metallic phase. The PDF for $x=0.4$ shows almost no JT distortion represented by the peak at 2.25 Å.

mined by integrating $4\pi r^2\rho_0 g(r)$ over the first peak up to the valley between the two peaks at $r=2.15$ Å, and multiplying by a factor involving the neutron-scattering lengths of the elements. Note that the peak at 1.95 Å includes only the Mn-O distances, so that the integration over this peak directly yields the number of short Mn-O bonds without any base-line subtraction.

In Fig. 6 the solid line labeled the ''small polaron model'' represents a linear relation between $N_{\text{Mn-O}}$ and the hole concentration x. It starts at 4 for $x=0$ representing JT distorted Mn^{3+} ions in $LaMnO_3$ and reaches 6 at $x=1.0$ representing Mn^{4+} in $SrMnO_3$ that has no JT distortion and has six Mn-O bonds with equal length. This linear relation assumes that the system is made of a mixture of Mn^{3+} and Mn^{4+} ions. A doped hole is localized within one octahedron as a Mn^{4+} ion, forming a single-site polaron. The experimental value of $N_{\text{Mn-O}}$ for $x=0$ is close to 4 as expected, and the room-temperature data are close to the single-site polaron line, indicating that in the PM phase holes are most likely localized as single-site polarons. The presence of single-site polarons in the PM state is in agreement with the theoretical prediction of entropic localization.[25] The previous PDF study[11] focused on the temperature dependence of the height of the peak at 2.75 Å. However, this peak includes not only the O-O distances within the MnO_6 octahedra but also significant contributions from La-O and Ca-O distances, clouding the analysis. The authors speculated on the nature of the polaron to be of a breathing type unrelated to the JT distortion by modeling the changes in the PDF through T_C, but it is difficult to obtain a conclusive result by modeling such small changes which are barely above the noise.

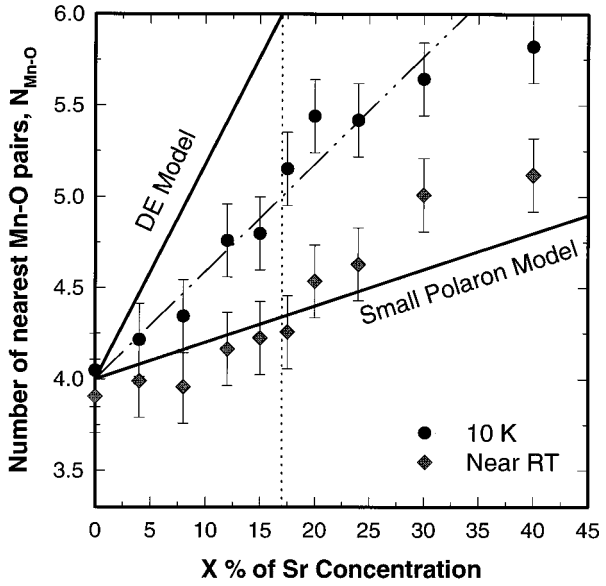

FIG. 6. The number of nearest O neighbors of Mn as a function of Sr doping at $T=300$ K (320 K for $x=0.2$, 350 K for $x=0.24$ and 0.3, in diamonds) and 10 K (circles). In the small polaron model the charges are localized at Mn^{4+} sites. At $T\approx$RT (room temperature), the data points are close to the ''small polaron model'' line. The data points at 30 and 40 % are slightly above the small polaron line because the data were collected slightly below T_C. The solid line labeled ''DE model'' represents the predictions by the Zener–de Gennes model, while the chained line is a linear fit to the 10 K data. This result suggests that at room temperature a hole forms a single-site small polaron (Mn^{4+}), but at $T=10$ K it is shared by about three octahedral sites forming a three-site polaron.

At $T=10$ K the composition dependence of $N_{\text{Mn-O}}$ in Fig. 6 (circles) is significantly above the single-site small polaron line. A fit to the data points, the chained line in Fig. 6, shows that a Mn coordination of 6 is reached at $\sim$35% of Sr doping with a slope that is about three times that of the single-site polaron line. This suggests that a hole is not localized on one site, but is spread on three Mn sites forming an extended three-site polaron. The formation of a three-site polaron may be related to the AFM ordering along the c axis or the orbital ordering in the plane. In $LaMnO_3$, once a spin is flipped on one Mn site it becomes parallel to the spins in the layers above and below, allowing easy passage of a hole among these three sites. Similarly an orbital rotation on one site would allow the hole to move easily to the neighboring two sites in the plane.

It should be noted that in the simple DE model as considered by de Gennes[7] the saturation of $N_{\text{Mn-O}}$ to 6 would be reached at the insulator-to-metal (I-M) transition at 17%, as also shown in Fig. 6 (''DE model''). However, at 17% the experimental value of $N_{\text{Mn-O}}$ at $T=10$ K is only around 5. This result and the PDF in Fig. 5 indicate that in the metallic phase up to 35% the structure is not uniform, and the local JT distortions are still present at some Mn sites. Moreover the linearity of the 10 K data up to $x=0.3$ in Fig. 6 suggests that the number of Mn sites without JT distortion per carrier is unchanged through the I-M transition. This result then appears to imply that the three-site polarons persist in the metallic phase.

However, that is an unusual proposition since the localized nature of polarons and metallic conduction are not mutually compatible. Usually as soon as the system becomes metallic charge carriers become delocalized and polarons disappear. How can local distortion and metallic conduction coexist? Before speculating on the physics of such a peculiar behavior it is useful to refer to the transport data of $La_{1-x}Sr_xMnO_3$ reported by Urushibara *et al.*[26] They show that the conductivity in the metallic phase depends strongly on composition. Just beyond the M-I transition the conductivity is relatively low even at low temperatures, and can be

fitted with a power law, $(x-x_C)^{\alpha}$ with $x_C=0.174$ and $\alpha\sim\frac{1}{2}$ up to $x\sim0.3$. The low conductivity is consistent with the local lattice distortion observed here in this composition range.

The results shown in Figs. 4–6 clearly suggest the presence of local JT distortion in the metallic phase. Such local JT distortions would locally split the e_g band, resulting in the full lower band. Consequently the local electron density at these Mn sites would be high, close to the one in the undoped $LaMnO_3$, and the doped holes would be repelled by the Mn sites with JT distortion. As the Sr concentration is decreased from $x=0.35$ the increase in the number of the JT distorted sites would lead to more scattering of the doped holes, therefore increased resistivity. A further decrease in x, thus a further increase in the concentration of the JT distorted sites, may lead to confinement of some doped holes and then to total localization and M-I transition.[27] Starting from the insulator side, on the other hand, the continuity of the $N_{\mathrm{Mn\text{-}O}}$ data through the M-I transition as x is increased suggests that this behavior could also be described in terms of connectivity of polaron networks.[28] This picture of a locally varying electronic structure in the metallic state that is strongly temperature dependent is consistent with the conductivity data discussed above and the results of photoemission,[29–31] thermopower,[13] and optical spectroscopy.[32]

The local variation of the electronic structure would also imply locally varying magnetic interaction.[33] One possible consequence is that even when the FM long-range order is established, locally antiferromagnetic (AFM) correlations can still be present,[2,34] which explains the unusual spin-wave damping.[35] Indeed exact diagonalization studies[36] have shown that in the pure DE model a homogeneous FM phase is unstable.

In conclusion this work has clearly shown that polaronic lattice distortions related to the local JT distortion exist in the PM and AFM as well as FM phases of $La_{1-x}Sr_xMnO_3$, and demonstrated that they play an important role in their transport and magnetic properties including the CMR phenomenon. In particular, the local lattice distortions are present even in the metallic state up to at least 35% of doping, in disagreement with the homogeneous picture of the double exchange model and other uniform mean-field models.

The authors are grateful to D. L. Price for advice regarding the GLAD spectrometer, and to Y. Tokura, A. Fujimori, A. J. Millis, J. B. Goodenough, K. A. Müller, M. Tachiki, S. Ishihara, S.-W. Cheong, Z.-X. Shen, M. Hundley, S. J. L. Billinge, S. D. Conradson, and T. Tyson for informative discussions. The work at the University of Pennsylvania was supported by the National Science Foundation Grant No. DMR96-28134, and at Los Alamos National Laboratory by U.S. Department of Energy. The IPNS is supported by the U.S. Department of Energy, Division of Materials Sciences under Contract No. W-31-109-Eng-38.

---

*Present address: Los Alamos National Laboratory, Los Alamos, NM 87545.

[1] G. H. Jonker and J. H. Van Santen, Physica (Amsterdam) **16**, 337 (1950).
[2] E. O. Wollan and W. C. Koehler, Phys. Rev. **100**, 545 (1955).
[3] J. B. Goodenough, Phys. Rev. **100**, 564 (1955).
[4] H. Jin *et al.*, Science **264**, 413 (1994).
[5] C. Zener, Phys. Rev. **81**, 440 (1951).
[6] P. W. Anderson and H. Hasegawa, Phys. Rev. **100**, 675 (1955).
[7] P. G. de Gennes, Phys. Rev. **118**, 141 (1960).
[8] A. J. Millis, P. B. Littlewood, and B. I. Shairman, Phys. Rev. Lett. **74**, 5144 (1995).
[9] M. F. Hundley *et al.*, Appl. Phys. Lett. **67**, 860 (1995).
[10] H. Y. Hwang *et al.*, Phys. Rev. Lett. **75**, 914 (1995).
[11] S. J. L. Billinge *et al.*, Phys. Rev. Lett. **77**, 715 (1996).
[12] T. A. Tyson *et al.*, Phys. Rev. B **53**, 13 985 (1996).
[13] W. Archibald *et al.*, Phys. Rev. B **53**, 14 445 (1996).
[14] G. Zhao *et al.*, Nature (London) **381**, 676 (1996).
[15] C. H. Booth *et al.*, Phys. Rev. B **54**, R15 606 (1996).
[16] P. G. Radaelli *et al.*, Phys. Rev. B **54**, 8992 (1996).
[17] T. Egami and S. J. L. Billinge, Prog. Mater. Sci. **38**, 359 (1994).
[18] B. H. Toby and T. Egami, Acta Crystallogr. Sect. A **48**, 336 (1992).
[19] H. L. Yakel, Acta Crystallogr. **8**, 394 (1955).
[20] J. F. Mitchell *et al.*, Phys. Rev. B **54**, 6172 (1996).
[21] J. J. Hamilton *et al.*, Phys. Rev. B **54**, 14 926 (1996).
[22] Note that the two experimental PDF's in Fig. 1 show no effect of the antiferromagnetic phase transition at 140 K (Ref. 2). This is because the magnetic correlation is more spread in space than the nuclear correlation due to the spatial extension of the $3d$ wave function. The magnetic correlation contributes only to the Mn-Mn peaks, and at 3.93 Å the magnetic PDF amplitude is estimated to be 0.02 $Å^{-3}$, almost at the level of the noise. The magnetic correlation does not at all affect the first Mn-O double peak.
[23] M. Hervieu *et al.*, Phys. Rev. B **53**, 14 274 (1996).
[24] P. Dai *et al.*, Phys. Rev. B **54**, R3694 (1996).
[25] H. Röder, J. Zang, and A. R. Bishop, Phys. Rev. Lett. **76**, 1356 (1996); **76**, 4987(E) (1996).
[26] A. Urushibara *et al.*, Phys. Rev. B **51**, 14 103 (1995).
[27] T. G. Perring *et al.*, Phys. Rev. Lett. **78**, 3197 (1997).
[28] It is most likely that when the polarons become connected holes would no longer be trapped in each polaron, and conducting paths will be formed. Conductivity then would be determined by some kind of dynamic percolative mechanism.
[29] T. Saitoh *et al.*, Phys. Rev. B **51**, 13 942 (1995).
[30] D. D. Sarma *et al.*, Phys. Rev. B **53**, 6873 (1996).
[31] D. S. Dessau, C. H. Park, and Z.-X. Shen (unpublished).
[32] Y. Okimoto *et al.*, Phys. Rev. Lett. **75**, 109 (1995).
[33] The spatial range of spin correlation can be larger than that of the charge correlation (Ref. 25), resulting in a different critical concentration (Refs. 2 and 26).
[34] A. W. Moudden *et al.*, Czech. J. Phys. **46**, 2163 (1996).
[35] T. G. Perring, Phys. Rev. Lett. **77**, 711 (1996).
[36] J. Zang *et al.* (unpublished); H. Röder *et al.* (unpublished).